Simulation of energetic particle injections associated with a substorm on August 27, 2001

Xinlin Li, T. E. Sarris,[1] D. N. Baker, and W. K. Peterson
Lab. for Atmospheric and Space Physics, University of Colorado, Boulder, USA

H. J. Singer
Space Environment Center, NOAA, Boulder, Colorado, USA

Received 24 July 2002; revised 20 September 2002; accepted 27 September 2002; published 3 January 2003.

[1] Discrete injections of energetic electrons and ions and their subsequent drift echoes were observed shortly after 0410 UT on August 27, 2001 by three geosynchronous satellites which were arrayed on the dayside. The GOES-8 spacecraft at geosynchronous orbit near local midnight, the four-satellite CLUSTER constellation also near local midnight. Concurrent and POLAR was at two hours after midnight. The observations from this suite of satellites provide the basis of information and constraints for us to model the particle injections. The simulations with test-particle simulations, reproduce both the observed electron and ion injections and subsequent drift echoes. Our simulation results support the idea that the energetic particle injections into the inner magnetosphere are a consequence of near-Earth magnetic reconnection. *INDEX TERMS:* 2720 Magnetospheric Physics: Energetic particles, trapped; 2744 Magnetospheric Physics: Magnetotail; 2764 Magnetospheric Physics: Plasma sheet; 2708 Magnetospheric Physics: Current systems (2409); 2730 Magnetospheric Physics: Magnetosphere—inner. **Citation:** Li, X., T. E. Sarris, D. N. Baker, W. K. Peterson, and H. J. Singer, Simulation of energetic particle injections associated with a substorm on August 27, 2001, *Geophys. Res. Lett.*, *30*(1), 1004, doi:10.1029/2002GL015967, 2003.

1. Introduction

[2] Energetic particle (10s–100s keV) injections are characteristic features of substorm onsets. Depending on the local time of the measurement, these injections can appear to be dispersionless, i.e., particle fluxes of different energies are enhanced at the same time. Early studies of the injection signatures observed at geosynchronous orbit [e.g., *Mauk and McIlwain*, 1974; *Konradi et al.*, 1975; *Mauk and Meng*, 1983] showed that they could be explained by the so-called "injection boundary" model proposed by *McIlwain* [1974].

[3] *Russell and McPherron* [1973] analyzed data from radially displaced satellites and found that a compressed magnetic field configuration associated with a substorm was propagating earthward at a speed of ~150km/s between 9 and 6.6 R_E. *Moore et al.* [1981] found dispersionless injections and associated magnetic signatures propagating earthward and they proposed an "injection front" model in which an injection corresponds to a compressional wave front that propagates earthward from a disturbance occurring in the magnetotail. Inspired by these results, *Li et al.* [1998, 1999] constructed a time-varying field model to simulate substorm particle injections. The time-varying fields were associated with the dipolarization and propagated toward the Earth at a constant speed. The simulation results, assuming initial kappa distributions with no spatial boundary, showed that dispersionless injections were caused by an electric field and a self-consistent magnetic field that propagate through the plasma, convecting the plasma inward and energizing it. Thus there is no need to invoke an "injection boundary" to explain the observed dispersionless injection.

[4] Using CRRES measurements, *Friedel et al.* [1996] found that dispersionless electron injections reached as far earthward as to L = 4.3. An intriguing feature of such deep penetrating injections is that they could remain dispersionless despite the fact that they travel slowly from geosynchronous orbit to CRRES at an average speed of 24 km/s [*Reeves et al.*, 1996]. *Sarris et al.* [2002] revised the model of *Li et al.* [1998] to make the propagation speed of the time-varying fields a function of radial distance. *Sarris et al.* [2002] reproduced the dispersionless electron injections observed both at geosynchronous orbit and at CRRES with the correct timing and flux enhancements.

[5] *Birn et al.* [1997, 1998] have investigated particle injections using geosynchronous observations and test-particle tracing in the fields generated by a three-dimensional MHD simulation of the magnetotail neutral line formation and dipolarization. Their test particle simulations can explain the initial rise of the particle injection at geosynchronous orbit at different local times near midnight. Furthermore, the MHD simulations show that substorm particle injections into the inner magnetosphere are a natural consequence of near-Earth reconnection. This conclusion was further supported by a more recent statistical study based on energetic particle measurements from fairly closely spaced geosynchronous satellites [*Thomsen et al.*, 2001].

[6] The work in this paper is motivated by a fortuitous arrangement of Earth-orbiting spacecraft associated with a relatively isolated magnetospheric substorm event on August 27, 2001 [*Baker et al.*, 2002].

2. Observations

[7] The locations of the spacecraft of interest are shown in the top panel of Figure 1. The CLUSTER constellation

[1]Currently visiting LASP, University of Colorado.

Copyright 2003 by the American Geophysical Union.
0094-8276/03/2002GL015967$05.00

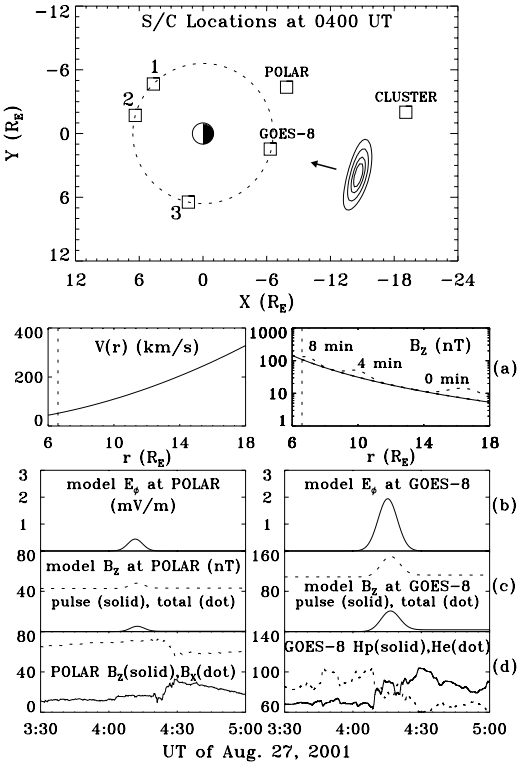

Figure 1. The top panel shows the spacecraft locations and the modeled pulse field. Numbers 1, 2 and 3 correspond to spacecraft LANL-97A, 1994-084 and 1991-080, respectively. The propagation speed of the pulse is plotted as a function of the distance in left panel (a). Right panel (a) shows the total magnetic field strength (dotted) and background dipole field (solid) at three time instants in the simulation at $\phi_0 = 160°$; Panels (b), (c), and (d) are self-explanatory.

of spacecraft were near its apogee ($\sim 19R_E$) and slightly post-midnight and were near the $Z_{GSM} = 0$ plane. At $\sim$0401 UT, all of the four CLUSTER spacecraft detected negative B_Z (southward magnetic field) and strong tailward flows in the plasmasheet that persisted for several minutes [*Baker et al.*, 2002]. About 8 minutes later, GOES-8 spacecraft at geosynchronous orbit near local midnight and at $Z_{GSM} \sim 1R_E$ measured a clear magnetic field dipolarization, right panel (d) of Figure 1. Energetic ion injections were first observed at satellite 3, which was closest to midnight at 0411 UT, and were subsequently observed at satellite 2 and satellite 1 as the ions drift westward (Figure 3); Energetic electron injections were detected at satellites 1, 2, and 3 as the electrons drifted eastward (Figure 2). Both the injected electron and ion populations were detected more than once by the same satellites. This is shown as multiple peaks in the flux measurements. Such features are referred to as drift echoes. These observations are consistent with magnetic reconnection occurring on the earthward side of the CLUSTER constellation and resulted in magnetic field dipolarization within a limited local time sector [*Baker et al.*, 1996] propagating toward the Earth. Concurrent measurements from POLAR, at $X_{GSM} \sim -9R_E$ and near 0200 LT and about 2 R_E above $Z_{GSM} = 0$ plane showed little change in the magnetic field and particle flux (data not shown here) between 0400–0410 UT (left panel (d) of Figure 1). GOES-10 at 1900 LT showed no obvious sign of dipolarization (data not shown here).

3. Model

[8] Mathematically, in the usual spherical coordinate system (r, θ, ϕ), where $r = 0$ at the center of the Earth, $\theta = 0°$ defines the equatorial plane and $\phi = 0°$ is at local noon, positive eastward, the electric field is given by:

$$\mathbf{E}_\phi = -\hat{e}_\phi E_0 (1 + c_1 \cos(\phi - \phi_0))^p \exp(-\xi^2) \qquad (1)$$

where $\xi = [r - r_i + v(r)\,(t - t_a)]/d$ determines the location of the maximum value of the pulse; $v(r) = a + br$ is the pulse-front velocity as a function of radial distance r; d is the width of the pulse; c_1 (> 0) and p(> 0) describe the local time dependence of the electric field amplitude, which is largest at ϕ_0; $t_a = (c_2 R_E/v_a)\,(1\text{-}\cos(\phi - \phi_0))$ represents the delay of the pulse from ϕ_0 to other local times; c_2 determines the magnitude of the delay, v_a is the longitudinal propagation speed of the pulse (assumed constant) and r_i is a parameter in the simulation that determines the arrival time of the pulse. In this report we present results with $\phi_0 = 160°$, $E_0 = 2mV/m$, $c_1 = 1$, $c_2 = 0.5R_E$, $a = 86.0\ km/s$, $b = 0.0145\ sec^{-1}$, $p = 8$, $v_a = 20\ km/s$, $r_i = 100R_E$, $d = 2.8 \times 10^8 m$ (after numerous runs, these parameters seemed to give the best results).

[9] Modeled fields $\mathbf{E}_\phi$ and $\mathbf{B_Z}$ are plotted as a function of time and at locations of POLAR and GOES-8 in Figure 1. It should be noted that our model fields are only applicable at the magnetic equator, while both POLAR and GOES-8 were off the magnetic equator. Nonetheless, the model perturbation field, in terms of initial rise time and magnitude, is consistent with the measurements, including GOES-10 measurements (not shown).

[10] We superpose this time-varying field on the background magnetic field and follow the particles using a

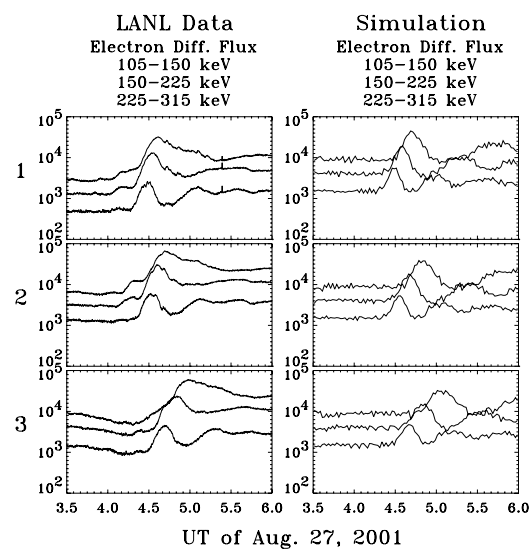

Figure 2. A comparison of LANL observations and simulation results for electrons.

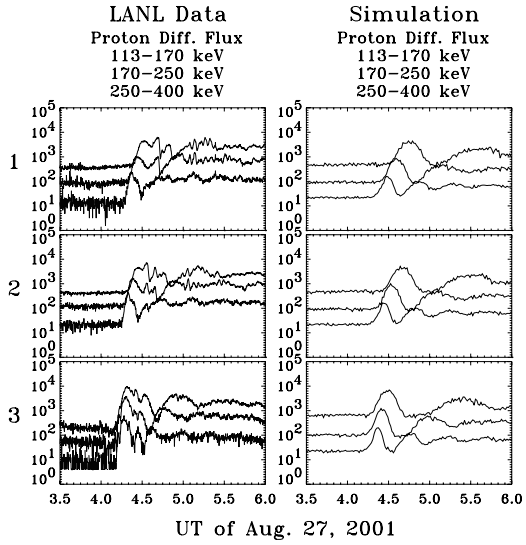

Figure 3. A comparison of LANL observations and simulation results for protons.

relativistic guiding center approximation for particles with $v_{\|} = 0$, [*Northrop*, 1963; *Li et al.*, 1993].

4. Results and Discussions

[11] We followed 500,000 electrons and 750,000 protons as they drifted on the equatorial plane in the combined pulse and background fields, recording their energy, arrival time, and radial distance as they passed various local times as well as their corresponding initial conditions. Both electrons and protons were initially distributed randomly in radial distance between 4 and $14R_E$ and at all local times in the equatorial plane. The initial energies start at 6 keV with a 5% increment, up to 361 keV for electrons and up to 418 keV for protons. In the post-processing stage, each particle is given a weight based on its initial position and energy to represent its contribution to the initial distribution. The initial energy distribution was a kappa distribution [*Vasyliunas*, 1968] with $\kappa = 1.8$ and $E_0 = 0.5$ keV for electrons and $\kappa = 2.7$ and $E_0 = 2.5$ keV for protons. These parameters are typical for a moderately active plasma sheet [*Christon et al.*, 1991] and similar to the ones used by *Birn et al.* [1997, 1998]. The initial particle distribution matches well the measurements at geosynchronous orbit before the injections, as shown in Figures 2 and 3. The initial radial dependence was given by

$$f_r = \left[\frac{(r_0 - a_0)^{nl}}{r_0^{ml}}\right] \Big/ \left[\frac{(a_{0d} - a_0)^{nl}}{a_{0d}^{ml}}\right], \qquad (2)$$

where $a_0 = 3$, $nl = 4$, $ml = 10$, $a_{0d} = 6$ for both electrons and protons. For protons, another factor is added:

$$f_r = f_r * \exp\left(-r_0^2/9.5^2\right) \qquad (3)$$

when r_0 is greater than 9.5 R_E.

[12] Thus, given an initial particle distribution, we can obtain particle fluxes and distributions at any location and time and can compare the simulation results with the LANL observations. The particle fluxes were summed over ±0.4 R_E at r = 6.6 R_E and plotted with a time resolution of 60 sec for protons and 90 sec for electrons. There are no new injections in the simulation.

[13] Figure 2 displays a comparison of energetic electron injections observed by LANL sensors (omni-directional) on three satellites at geosynchronous orbit with a time resolution of 10 sec [*Belian et al.*, 1992] and the simulation, in which the detectors' response has been incorporated. The dispersion feature, drift echo, the width and shape of the fluxes are more or less reproduced. The electrons in the simulation seem to drift faster and more coherently than the measurements since we only trace 90° pitch angle particles at magnetic equator in the simulation. The simulated electron enhancements fall off more rapidly than those in the observations. This is because of the rapid falloff B_z in the model as compared to the observations (panel (c) and (d) of Figure 1), which is also the reason for the more rapid falloff of the simulated proton enhancements to be discussed below.

[14] Figure 3 shows a similar comparison but for protons (most ions are protons for this event [*Baker et al.*, 2002]). In the simulation, the identical model field is used but the initial particle distribution is different from the electrons, as described earlier.

[15] Figure 4 shows the profile of initial positions of particles that are injected into geosynchronous orbit. For a given energy channel each bar represents the percentage of all recorded particles that came from the corresponding distance. Bars are plotted every 0.5 R_E in L, and the sum of all bars for each energy channel equals one, or 100%. The extent of the region is different for each energy channel but all of them are continuous, and no particles initially located beyond 11.5 R_E can be brought to geosynchronous orbit in the simulation. The first adiabatic invariant, μ, is conserved in the model. In the real situation, the magnetic field configuration can be much more complicated, μ may not remain as a constant in large L, especially in the case of high-energy ions. Nonetheless, a charged particle always gains energy when it is brought from a weaker field region to a stronger field region, vice-versa. It should also be noted that our background magnetic field is a dipole, $B_E \sim 1/r^3$ and that

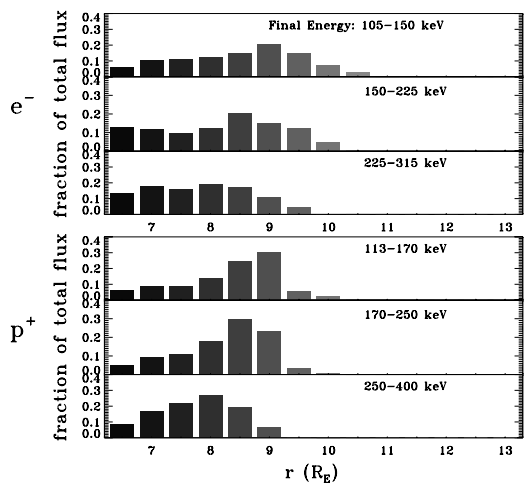

Figure 4. Profiles of the initial positions of all the electrons (upper panel) and protons (lower panel) that are injected to geosynchronous orbit in the simulation. The gray scale of the bar is proportional to the energy for the same panel: darker means higher energy particles.

the real magnetic field does not decay as fast versus distance. Thus, to gain the same amount of energy, the injected particles measured at geosynchronous orbit may need to come from even farther away than Figure 4 suggests.

[16] The measured proton fluxes have multi-peaks during the initial injection while measured electrons do not, see Figures 2 and 3. The simulated injections do not show any multi-peaks during the initial injection for both protons and electrons. It is known that the multi-peak feature during the initial injection can be due to the nonuniform distribution of the source population [*Li et al.*, 1998]. Thus, it seems that the actual source protons in the plasmasheet were not uniform and were more dynamic than the source electrons.

[17] In the simulation, it takes about 8 min for the pulse field to propagate from 18 to 6.6 R_E, which is consistent with the time delay of ~8 min between the measured dipolarization at GOES-8 and the magnetic reconnection detected by CLUSTER [*Baker et al.*, 2002]. However, our test-particle simulation cannot address the initiation of substorms. There is still some uncertainty regarding exactly when the dipolarization, such as modeled here, is initiated and how fast it propagates toward the Earth given that a magnetic reconnection onset takes place in the tail.

[18] When a given satellite measures the first injected particles depends on: (1) relative position to the injection site, (2) particle species (electrons and ions drift in opposite directions), and (3) particle energy (gradient-B drift is energy dependent). In order to reproduce the injections of both protons and electrons measured by three satellites at geosynchronous orbit, we have tried to place the pulse field coming at different local times and at the same time keeping the magnetic field matching observations at GOES-8, GOES-10, and POLAR. We found that having the pulse coming toward the Earth at 2240 LT, $\phi_0 = 160°$, gives the best results. When the pulse was coming at 0200 LT, the initial rise of the highest electron channel (225–315 keV) was ~4 min ahead of the one presented in Figure 2 and the initial rise of the highest proton channel (250–400 keV) was delayed by ~3 min compared to the one in Figure 3. We also located the pulse at 2120 LT and then the highest electron channel was delayed ~2 min while the highest proton channel was ~1.5 min ahead. Also observations at GOES-8, GOES-10, and POLAR put a strict restraint on local time dependence of the pulse (parameter p in equation (1)).

[19] On the other hand, CLUSTER clearly detected the magnetic reconnection signature when it was nearly post midnight [*Baker et al.*, 2002], which suggests that reconnection extends over a large local time in the middle magnetotail and the pulse field associated with the reconnection is still limited in local time when reaching near geosynchronous orbit.

5. Conclusions

[20] The essence of our model is the following: Associated with the dipolarization, there is an inductive electric field, pointing predominantly westward, which will transport particles toward the Earth via $\mathbf{E} \times \mathbf{B}$ drift and energize them via betatron acceleration, which leads to the observed injections. This model has been used to simulate energetic particle injections associated with substorms [*Li et al.*, 1998; *Sarris et al.*, 2002].

[21] The major results are: (1) there are more observational constraints on the model perturbation fields; (2) both the electron and proton injections and subsequent drift echoes are reproduced. These results further demonstrate the merit of the model.

[22] Our simulation results also support the idea that energetic particle injections into the inner magnetosphere are a consequence of near-Earth reconnection as interpreted by *Baker et al.* [2002].

[23] **Acknowledgments.** We thank S. Monk for programming efforts and C. T. Russell for providing POLAR/magnetic field data. We appreciate the LANL and CLUSTER science teams' effort to make the data available. This work was supported by NASA grants (NAG5-9421 and -10474) and NSF grants (ATM-9909357 and -9901085)

References

Baker, D. N., et al., Neutral line model of substorms: Past results and present view, *J. Geophys. Res.*, *101*, 12,975, 1996.

Baker, D. N., et al., Timing of magnetic reconnection initiation during a global magnetospheric substorm onset, *Geophys. Res. Lett*, in press, 2002.

Belian, R. D., et al., High-Z energetic particles at geosynchronous orbit during the great solar proton event series of October 1989, *J. Geophys. Res.*, *97*, 16,897, 1992.

Birn, J., et al., Substorm ion injections: Geosynchronous observations and test particle orbits in three-dimensional dynamics MHD fields, *J. Geophys. Res.*, *102*, 2325, 1997.

Birn, J., et al., Substorm electron injections: Geosynchronous observations and test particle simulations, *J. Geophys. Res.*, *103*, 9235, 1998.

Christon, S. P., et al., Spectral characteristics of plasma sheet ion and electron populations during disturbed geomagnetic conditions, *J. Geophys. Res.*, *96*, 1, 1991.

Friedel, R. H. W., A. Korth, and G. Kremser, Substorm onsets observed by CRRES: Determination of energetic particle source regions, *J. Geophys. Res.*, *101*, 13,137, 1996.

Konradi, A., et al., Substorm-injected protons and electrons and the injection boundary model, *J. Geophys. Res.*, *80*, 543, 1975.

Li, X., I. Roth, M. Temerin, J. Wygant, M. K. Hudson, and J. B. Blake, Simulation of the prompt energization and transport of radiation particles during the March 23, 1991 SSC, *Geophys. Res. Lett.*, *20*, 2423, 1993.

Li, X., D. N. Baker, M. Temerin, G. Reeves, and R. Belian, Simulation of Dispersionless Injections and Drift Echoes of Energetic Electrons Associated with Substorms, *Geophys. Res. Lett.*, *25*, 3763, 1998.

Li, X., D. N. Baker, M. Temerin, G. Reeves, and R. Belian, Auroral Substorm Origin Far Out in Magnetotail, Dispersionless Injection Simulations Suggest, EOS, p. 405, Sept. 7, 1999.

Northrop, T. G., The adiabatic motion of charged particles, Interscience Publishers, New York, 1963.

Mauk, B., and C. McIlwain, Correlation of Kp with the substorm injected plasma boundary, *J. Geophys. Res.*, *79*, 3193, 1974.

Mauk, B., and C.-I. Meng, Characterization of geostationary particle signatures based on the "injection boundary" mode, *J. Geophys. Res.*, *88*, 3055, 1983.

McIlwain, C., Substorm injection boundaries, *Magnetospheric Physics*, edited by B. M. McCormac, p. 143, D. Reidel, Hingham, Mass., 1974.

Moore, T. E., et al., Propagating substorm injection fronts, *J. Geophys. Res.*, *86*, 6713, 1981.

Reeves, G. D., et al., Radial propagation of substorm injections, International Conference on Substorms-3, *ESA SP-339*, 579, 1996.

Russell, C. T., and R. L. McPherron, The magnetotail and substorms, *Space Sci. Rev.*, *15*, 205, 1973.

Sarris, T. E., X. Li, N. Tsaggas, and N. Paschalidis, Modeling Energetic Particle Injections in Dynamic Pulse Fields with Varying Propagation Speeds, *J. Geophys. Res.*, 107, 10.1029/2001JA900166, 2002.

Thomsen, M. F., et al., Two-satellite observations of substorm injections at geosynchronous orbit, *J. Geophys. Res.*, *106*, 8405, 2001.

Vasyliunas, D. J., A survey of low-energy electrons in the evening sector of the magnetosphere with OGO 1 and OGO 3, *J. Geophys. Res.*, *73*, 2839, 1968.

D. N. Baker, X. Li, and W. K. Peterson, LASP/CU, 1234 Innovation Drive, Boulder, CO 80303-7814, USA. (lix@lasp.colorado.edu)

T. E. Sarris, Department of Electrical Engineering, Demokritus University of Thrace, Vas. Sofias 1, 67100 Xanthi, Greece.

H. J. Singer, NOAA, 325 Broadway, Boulder, CO 80303, USA.